UCRL 8980

UNIVERSITY OF CALIFORNIA

Ernest O. Lawrence Radiation Laboratory

POLARIZATION OF BREMSSTRAHLEN

TWO-WEEK LOAN COPY

This is a Library Circulating Copy which may be borrowed for two weeks. For a personal retention copy, call Tech. Info. Division, Ext. 5545

DISCLAIMER

This document was prepared as an account of work sponsored by the United States Government. While this document is believed to contain correct information, neither the United States Government nor any agency thereof, nor the Regents of the University of California, nor any of their employees, makes any warranty, express or implied, or assumes any legal responsibility for the accuracy, completeness, or usefulness of any information, apparatus, product, or process disclosed, or represents that its use would not infringe privately owned rights. Reference herein to any specific commercial product, process, or service by its trade name, trademark, manufacturer, or otherwise, does not necessarily constitute or imply its endorsement, recommendation, or favoring by the United States Government or any agency thereof, or the Regents of the University of California. The views and opinions of authors expressed herein do not necessarily state or reflect those of the United States Government or any agency thereof or the Regents of the University of California.

UCRL-8980
Physics and Mathematics
TID-4500 (15th Ed)

UNIVERSITY OF CALIFORNIA
Lawrence Radiation Laboratory
Berkeley, California

Contract No. W-7405-eng-48

POLARIZATION OF BREMSSTRAHLEN

John M. Dudley

(Thesis)

November 13, 1959

Printed for the U. S. Atomic Energy Commission

POLARIZATION OF BREMSSTRAHLEN

Contents

Abstract 3
I. Introduction 4
II. Apparatus
A. Reasons for Choice of Apparatus 7
B. Setup and Collimation 8
C. Target and Sweep Mechanisms 10
D. Detector 15
III. Experimental Details
A. Choice of Basic Experimental Conditions: Detection Method, Energy, and Target 20
B. Detection 21
C. Scanning and Analysis 23
IV. Theoretical Remarks
A. Plausibility Argument for Polarization 26
B. Remark on Plane vs Circular Polarization 29
C. The Theoretical Literature
1. The Intrinsic Cross Sections 30
2. Scattering in the Target: Mathematical Preliminaries and Definitions 34
3. Scattering in the Target: Published Material. 40
D. The Calculation of Expected Polarization Including Scattering 41
V. Results 45
VI. Acknowledgments 47
References 48

POLARIZATION OF BREMSSTRAHLEN

John M. Dudley

Lawrence Radiation Laboratory
University of California
Berkeley, California

November 13, 1959

ABSTRACT

The partial polarization of bremsstrahlen originating from a well-collimated beam of electrons incident upon a thin radiating target has been observed. Detection of the polarized radiation was by the angular dependence of deuteron photodisintegration. A survey of the currently available theoretical treatments of the phenomenon is presented; a modification of the theory to include the effect of multiple scattering in the radiator is suggested. For incident electron total energy E_0 = 25.5 Mev, the fractional degree of plane polarization of bremsstrahlen from a 1-mil aluminum radiator, with photon energies in a band about 5 Mev, observed at an angle 1.5 mc^2/E_0 radians from the center of the bremsstrahlen beam, is found to be $\Pi = 0.44 \pm 0.22$, in agreement with the modified theoretical prediction, $\Pi = 0.45$.

I. INTRODUCTION

Within the last decade there has been increasing interest in the state of polarization of bremsstrahlen for two reasons: polarized radiation may be the result or the initiator of an experiment. Detection of such radiation offers a possible experimental determination of the state of polarization of initiating electrons that come from weak-interaction processes; as the initiator of a reaction, polarized radiation provides a possible additional known condition in the study of electromagnetically induced processes. We have attempted to investigate the polarization of bremsstrahlen from unpolarized electrons for the latter reason, and because of a general interest in the phenomenon. In practically all the experiments on photon-induced nuclear reactions an average has been taken over the possible states of polarization of the incident photons. It is apparent that if one were able to use photons of known polarization, additional information could be obtained.

Experimental investigations of the degree of plane polarization of bremsstrahlen beams in the energy region of interest to us, where the initiating electron energy is 10 to 30 Mev, have been reported by several authors. All but one used deuterium photodisintegration detection in one form or another, and all used betatrons as sources of photons. Phillips obtained results that indicated a second plane of prominent polarization as well as the one expected;[1] Muirhead and Mather's results were inconclusive;[2] Tzara reported an unexpectedly high degree of polarization;[3] Jamnik and Axel detected polarization by means of the angular dependence of the scattering of polarized photons, and obtained results in accord with the theory, within the limitations of their method.[4] In the energy region at and below 1 Mev, Motz and Placious have exhibited qualitative agreement with theory.[5]

The experiment described here attempts to remove some of the ambiguities inherent in the work referred to above. A preliminary account of it has been published.[6]

Before we discuss the experiment in detail, we should define the most fundamental terms involved. Theoretical investigations (considered in Section IV) predict that the bremsstrahlen produced

when energetic electrons strike a very thin target are partly plane polarized, in the ordinary sense of polarization of visible light, over nearly the whole bremsstrahlung energy spectrum and over a relatively large range of angles θ in the beam. The maximum polarization is predicted to be at a characteristic angle $\theta_0 \equiv mc^2/E_0$, where E_0 is the total energy of the initiating electron, and the electric vectors are predicted to be predominantly in the angular range labeled "$\perp$" in Fig. 1. For thicker targets, the peak of polarization of the radiation is broadened, displaced to larger values of θ, and reduced by the effect of multiple scattering of electrons in the radiator.

In this work, the fractional polarization observed at an angle θ in the laboratory frame (shown in Fig. 1) is defined by

$$\Pi(\theta, E_0, k, T) = \frac{\Sigma_\perp(\theta, E_0, k, T) - \Sigma_{||}(\theta, E_0, k, T)}{\Sigma_\perp(\theta, E_0, k, T) + \Sigma_{||}(\theta, E_0, k, T)},$$

where $\Sigma_\perp(\theta, E_0, k, T)$ is the whole-target cross section per unit solid angle for production of bremsstrahlen of the following characteristics: the initiating electron has total energy E_0; the photon observed has an energy in a band about k, and its electric vector is perpendicular to the plane containing the paths of the incident electron and the photon. The radiation is produced in a target of given material and of thickness T. The quantity $\Sigma_{||}(\theta, E_0, k, T)$ is similarly defined for a photon with its electric vector parallel to the plane of production. The value of the polarization does not depend upon the azimuthal angle about the center of the bremsstrahlung beam, but the significance of $\Sigma_\perp$ and $\Sigma_{||}$ does. The plane "$\perp$" is everywhere tangent to the surface of the cone of half-angle θ centered on the (extended) path of the incident electron.

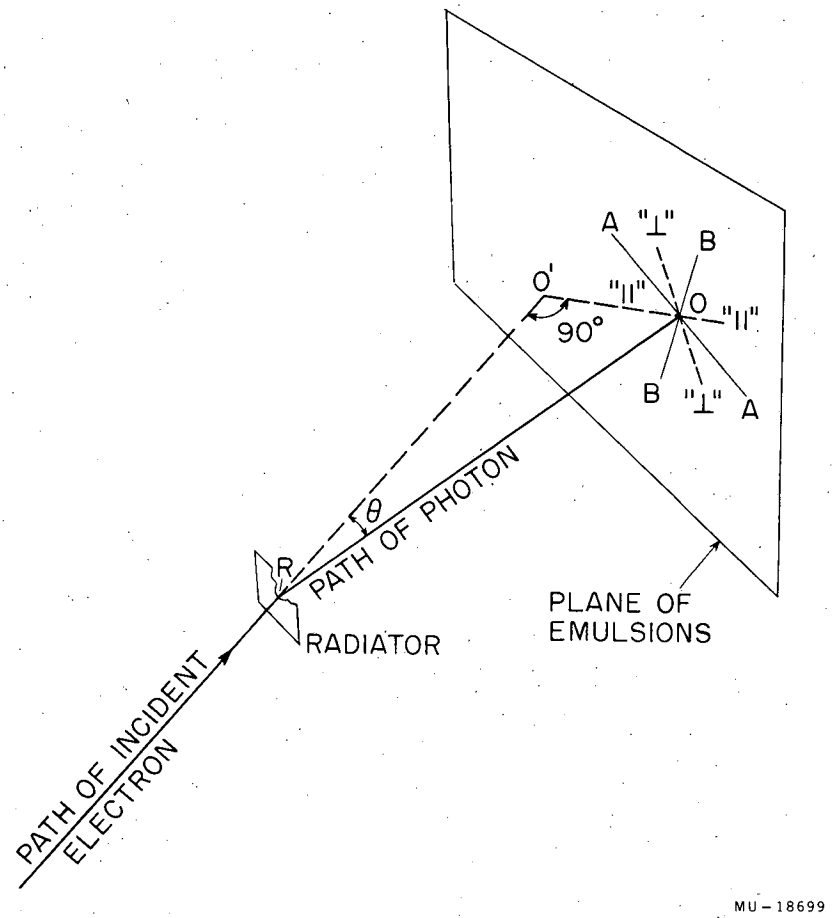

Fig. 1. Geometry of bremsstrahlung event and deuterium photoproton tracks. The intersection of the plane of emulsions, which is perpendicular to the path of the incident electron, with the plane of emission (O'RO) is along O'O. The quadrants (AOB) in the plane of emulsions are centered on the two mutually perpendicular directions "⊥" and "||". RO' is the extended path of the incident electron.

II. APPARATUS

This investigation was carried out at the Stanford University Mark II 35-Mev linear electron accelerator, whose collimated beam struck a thin aluminum target, producing bremsstrahlen. The electrons, after passing through the target, were swept aside magnetically and the bremsstrahlen struck the detector.

A. Reasons for Choice of Apparatus

Most of the early attempts to investigate the polarization of bremsstrahlen were made by using betatrons. Invariably in circular machines the complementary problems of small-angle scattering or of multiple traversals of the target arise. In many such machines the electron beam at maximum energy spirals slowly inward, making a large number of turns, to strike the target, losing energy gradually by synchrotron radiation. Other designs use a beam-expander pulse to cause the electrons to spiral outward to the target. Consequently, in either case, the initial angle of impact on the target is well defined. However, if the target is thick, the multiple scattering and repeated bremsstrahlung processes in a single traversal of the target together decollimate the beam. On the other hand, if the target is thin enough to eliminate these two effects, the electrons on traversing the target lose so little energy that there is a good chance that they may stay approximately in a stable orbit and come around to strike the target again, this time at an indeterminate angle. Such repeated traversals produce an effect equivalent to that of a thick target. Either process spoils the precise collimation of the incident beam required for this experiment.

Obviously these difficulties would be eliminated if the precisely collimated beam of a linear accelerator could be used as the initiator of the bremsstrahlen. By the generous cooperation of Stanford University, the Mark II accelerator was made available for our use. This machine, together with the associated double-focusing and collimating equipment, can produce an electron beam whose

energy can be chosen at will up to a maximum of 35 Mev, and whose energy spread at the chosen energy can be limited to as little as 1/4 %. The magnetic double-focusing system allows great control of the trajectory of the emergent beam. A similar system has been described by Panofsky and McIntyre.[7] The theory of such systems has been published by Camac.[8]

B. Setup and Collimation

The only serious limitation on the focusing lies in the interdependence of the horizontal, vertical, and energy focus points, so in most experiments with this machine (and in this one in particular) a compromise must be arrived at. Although ideally, for the purposes of this experiment, it might have been possible to restrict the convergent angle of the beam at the target, either horizontally or vertically, more than we did, we were somewhat limited by the physical size of the experimental area. We used the full length of the room from exit port to shielding wall, and chose the horizontal and vertical focal points in such a way that the convergence angles at the radiating target in both dimensions were within satisfactory limits and that there was sufficient space between radiator and detector for the bremsstrahlen beam to spread enough for conveniece in scanning (see Fig. 2). The electron beam was collimated at the entrace to the double-focusing system by a 3/16-in.-diameter collimator; at the target the electron beam spot was rougly elliptical in cross section, 3/8 in. wide and 3/16 in. high; the horizontal convergence half angle was $\leqslant \theta_0/4$, and the vertical convergence half angle was $\leqslant \theta_0/8$. To allow sufficient beam intensity for reasonable exposure times, we chose the initial electron kinetic energy T_0 = 25 Mev ± 1%.

The beam from the exit port of the double-focusing and collimating apparatus passed along the axis of a 4-in. segmented brass tube which, although evacuated with an auxiliary pump, was an integral part of the accelerator vacuum system. To permit experimental adjustment and checking of the electron beam trajectory, this tube was made in three segments: a long permanent segment, with two

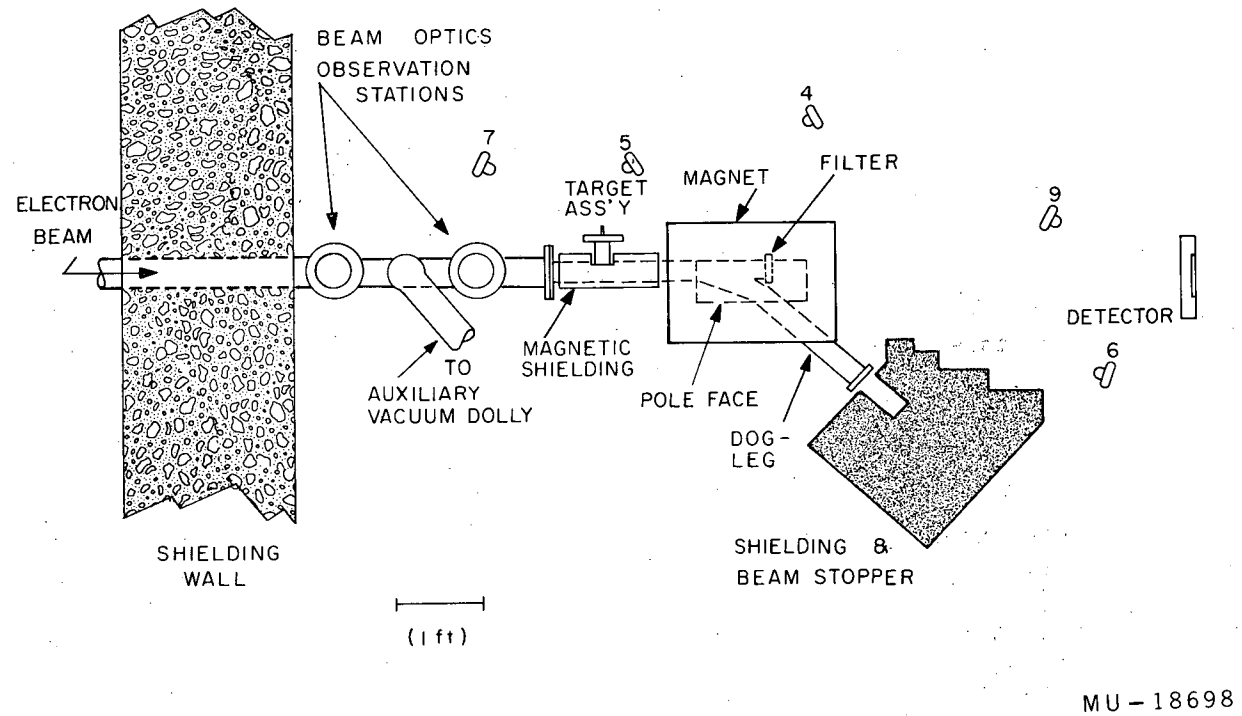

Fig. 2. Schematic top view of apparatus. Camera angles for other figures shown for orientation.

tubulations on top (plus the vacuum connection), placed before the desired focal point; a second shorter section whose one tubulation was placed at the expected focal point; a third longer section with two more tubulations behind that. All these tubulations were capped with Lucite plates, in each of which was set a Wilson seal through which ran a rod controlling the vertical position of a paddle coated with fluorescent paint. To check the position of the beam at each of these five stations, we lowered the paddle to intercept the beam and photographed the fluorescing spot with a Land camera (Fig. 3). When not in use to determine the electron beam trajectory, the paddles were withdrawn into the tubulations. When the trajectory had been determined the temporary straight brass tubes were removed and the target assembly, dog-leg (described below), and sweep magnet installed. Thus, a running check on the beam trajectory could be made during the experiment at the two prefocus tubulations remaining (Figs. 4 and 5).

C. Target and Sweep Mechanisms

Because we wished to have a pure bremsstrahlen beam, uncontaminated by the electrons which passed through our thin target (electrons, if allowed to strike the detector plates, would expose them far more than the electromagnetic radiation of interest), it was necessary to sweep the posttarget region magnetically. The electrons after having passed through the target were directed through an offset (dog-leg) tube and collected during the initial runs in a well shielded Faraday cup (see Fig. 6), by which means we were able to integrate the total beam current for an exposure. The trajectory of the electrons in the sweep magnet was checked by the wire method. In the later stages of the experiment, because of the high neutron flux generated in the Faraday cup (the neutrons, if they were to strike the plates, might well produce knock-on protons indistinguishable from the ones of interest), the Faraday cup was replaced by a carbon beam stopper, shielded with iron and paraffin, whose neutron production was appreciably less.

The dog-leg section of the vacuum system was fitted at the target position with a side tubulation capped with a Lucite plate through

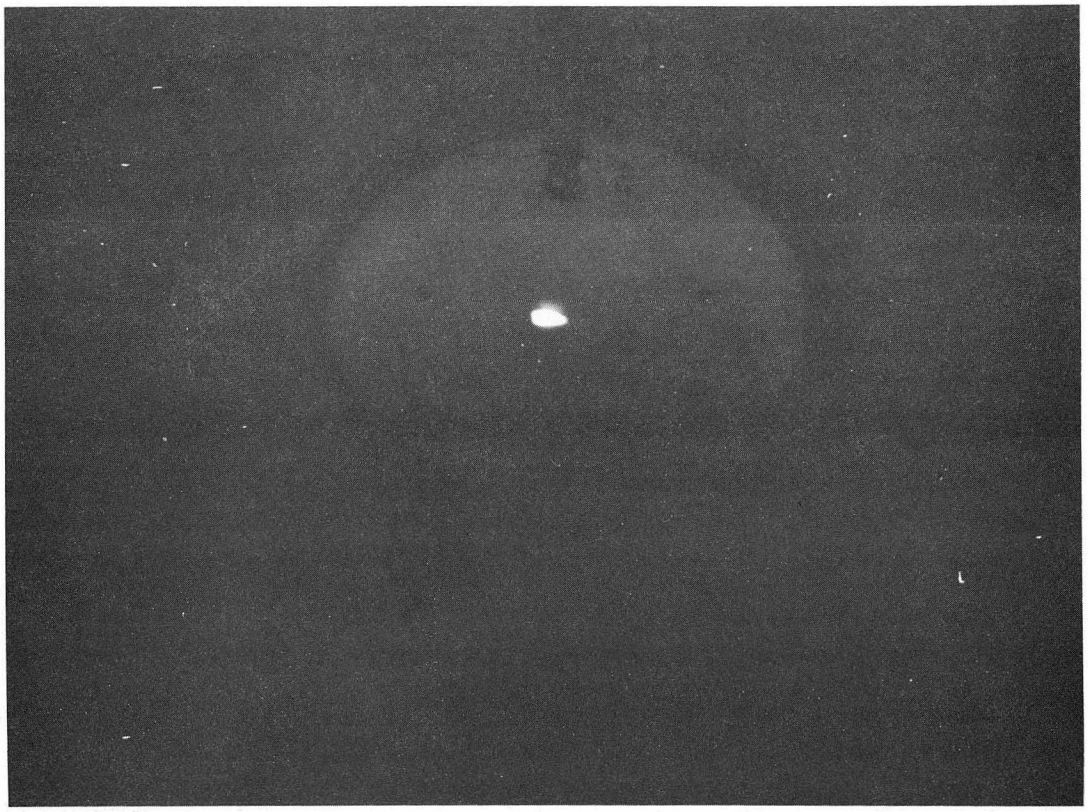

ZN-2282

Fig. 3. Land camera picture of beam spot at the target position (taken during line-up). The fiducial holes demarcate a 1-by-2-inch rectangle in the plane of the paddle.

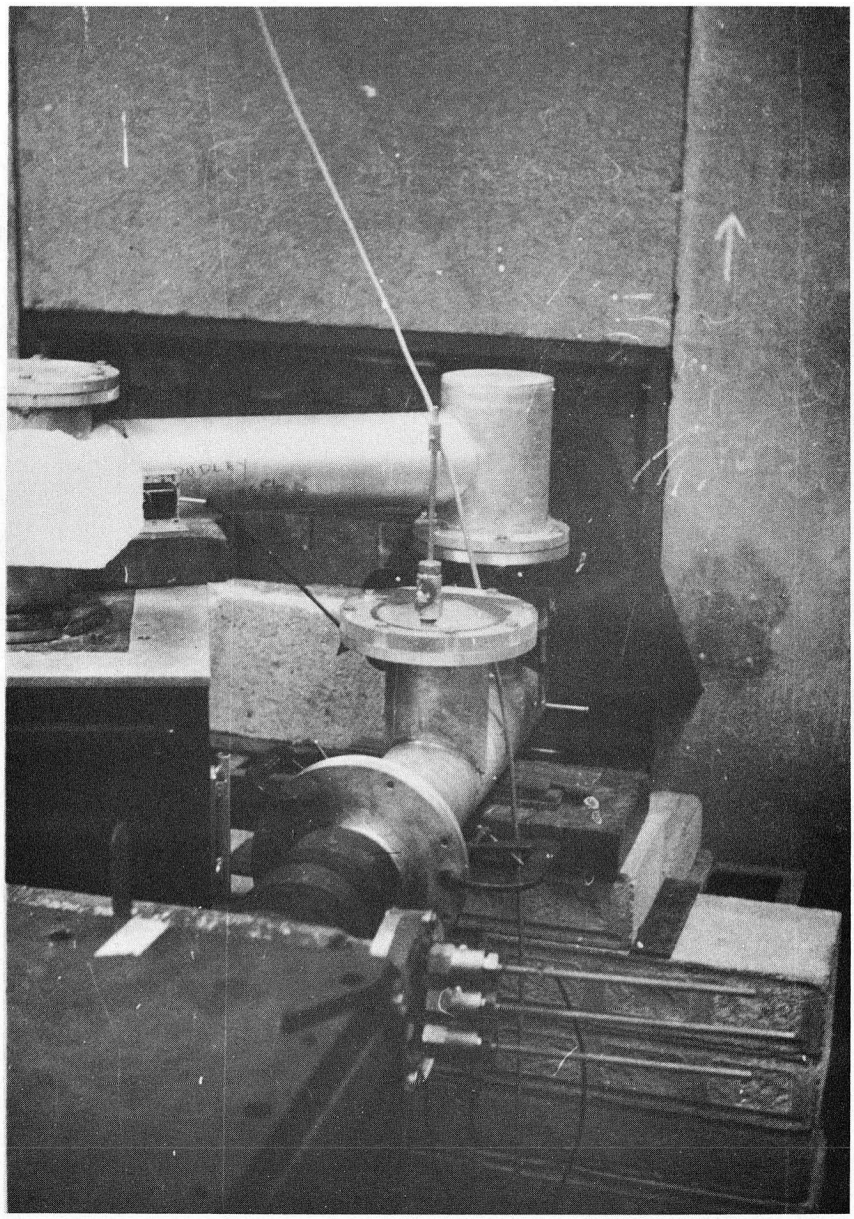

ZN-2283

Fig. 4. Beam-optics check station in center of picture. The paddle is withdrawn into the tubulation (control rod up).

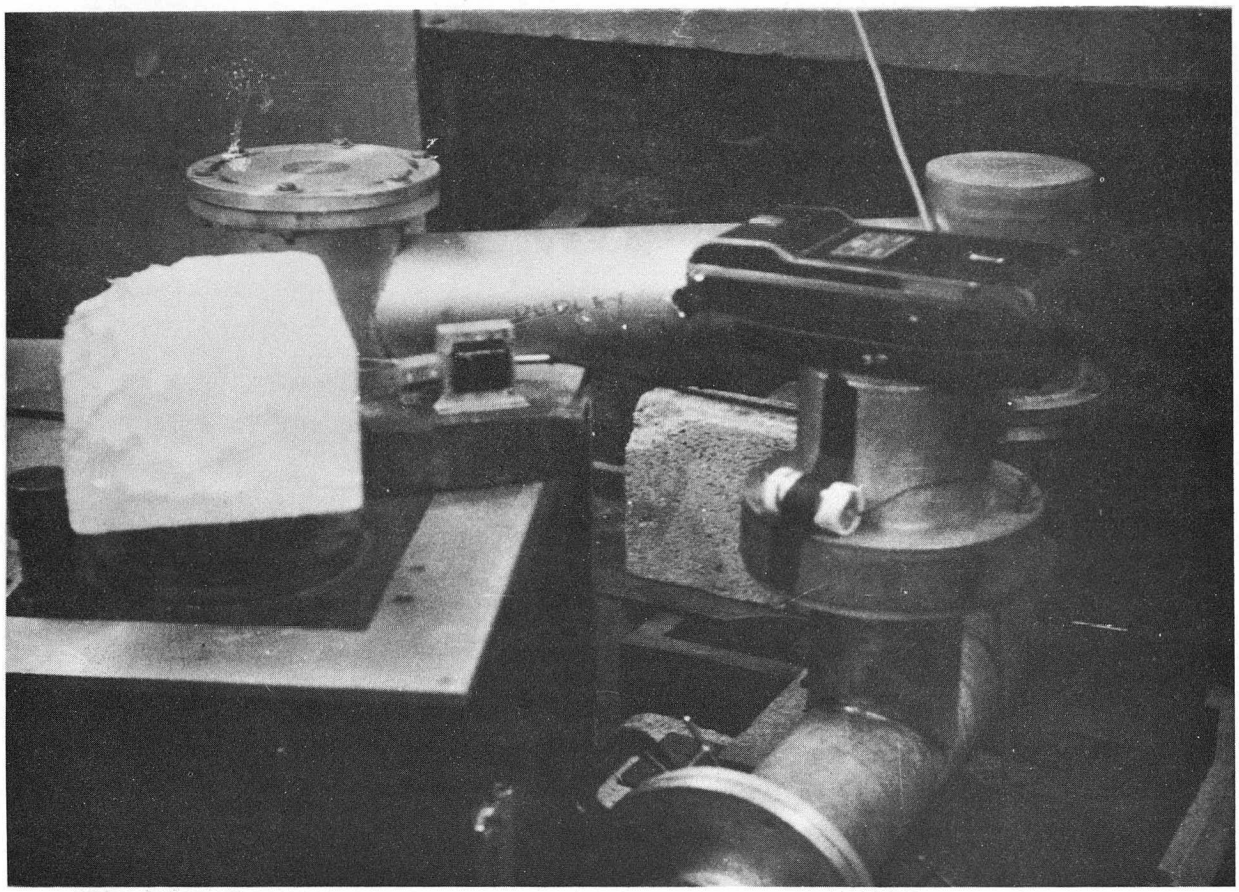

ZN-2285

Fig. 5. Setup for beam optics check.

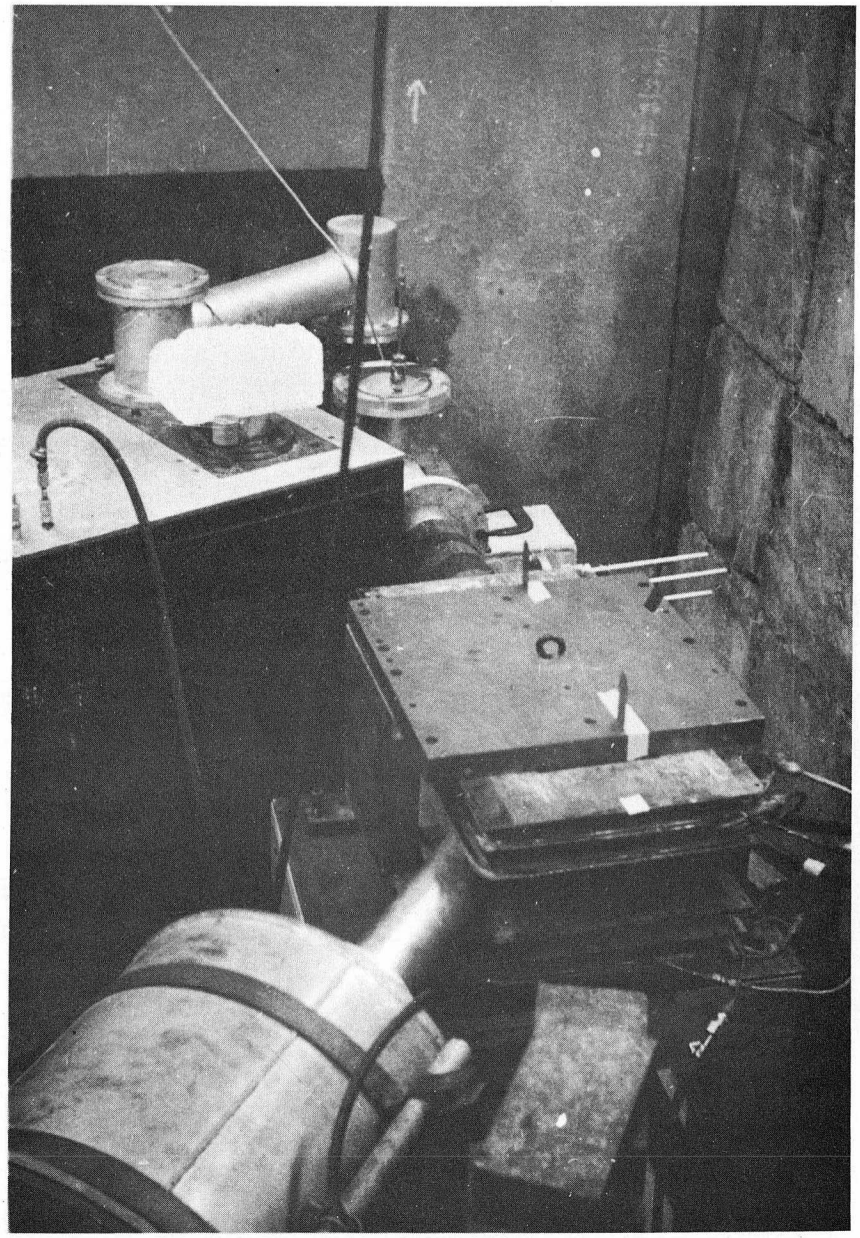

ZN-2286

Fig. 6. Complete apparatus. Beam centerline from left center to lower right. Faraday cup at lower left; auxiliary vacuum dolly at far left center; magnet at right center.

which ran three rods in Wilson seals (Fig. 7). Any or all of these rods could be withdrawn into the tubulation or thrust out into the main tube. At the end of the upper rod there was a 2-in.-diameter thin aluminum ring which supported the 1-mil aluminum foil target. The bottom rod was fitted with an identical thin aluminum ring left blank. This served as a dummy for the target. The middle rod bore at its end a glass microscope slide (see Fig. 8). By these means we were able to expose "target-in, target-out," and at the end of each run determine precisely the small area of the target which was struck by the incident electrons by exposing in place of the target the microscope slide, which was darkened at the point where the electrons passed through. This latter test confirmed that in all cases the electron optics remained stable and the supporting ring for the target was completely out of the beam. The target region was shielded with iron from the stray field of the near-by sweep magnet, lest the electron trajectory near the target be disturbed (Fig. 7).

The bremsstrahlen emerged from the evacuated system through an aluminum window and a thin lead filter (3/16 in.) -- which was introduced to reduce low-energy background--and passed through the intervening air to the detector. A portion of the deflecting field for the main beam of electrons was used to remove secondary electrons produced in the window and filter (Fig. 2).

D. Detector

The detector (Fig. 9) was constructed as follows: six 200-μ Ilford C.2 emulsions on 1-by-3-inch glass supports were arranged side by side to form a 3-by-6-inch rectangle. A second set of six plates was arranged identically. A double-decker sandwich of three thin stainless steel foils and these two sets of plates was mounted perpendicular to the axis of the beam of photons, with the emulsion side of each set of plates facing toward the radiator. The set of six plates that was to be nearer the radiator was soaked for several hours prior to exposure in D_2O; the set directly behind it in the sandwich was similarly loaded with H_2O. During exposure the plates in both sections

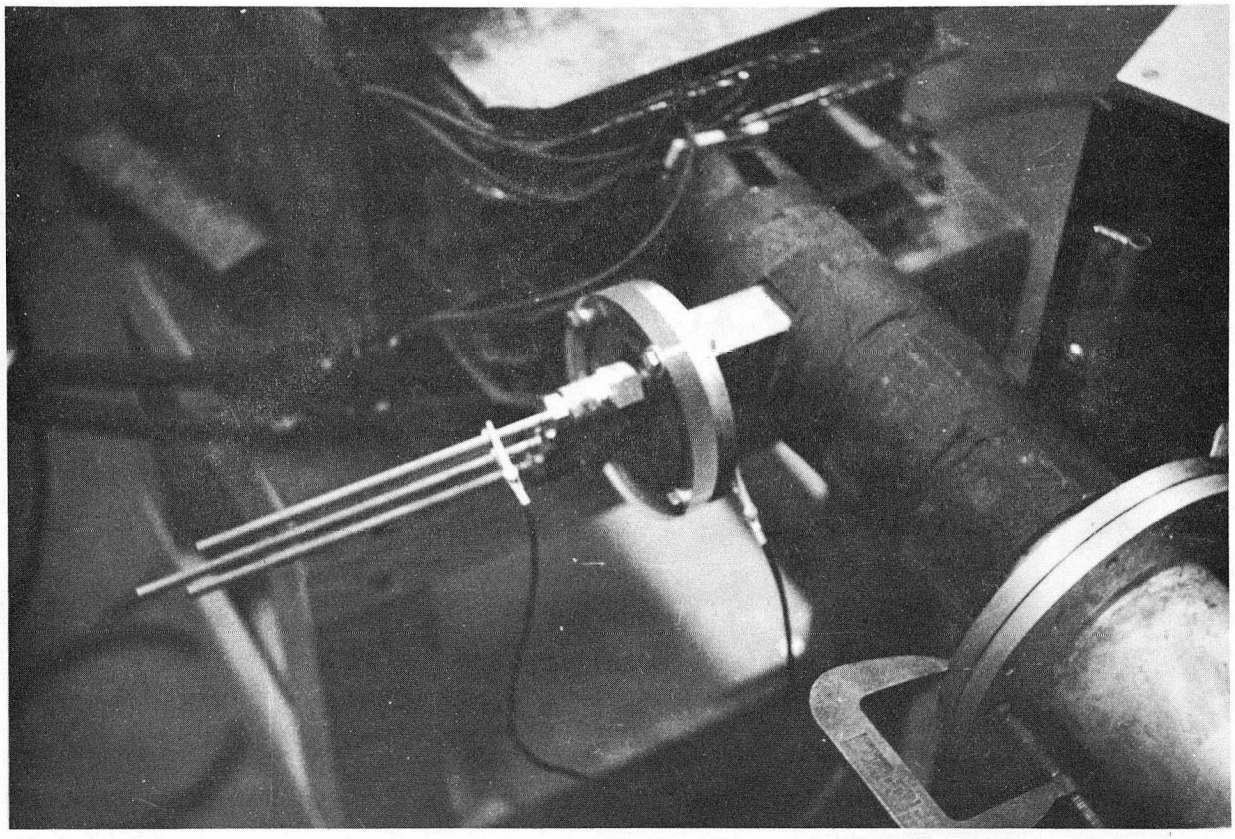

ZN-2280

Fig. 7. Target assembly in position. The dark color of the magnetic shielding in the target region contrasts with the bright brass.

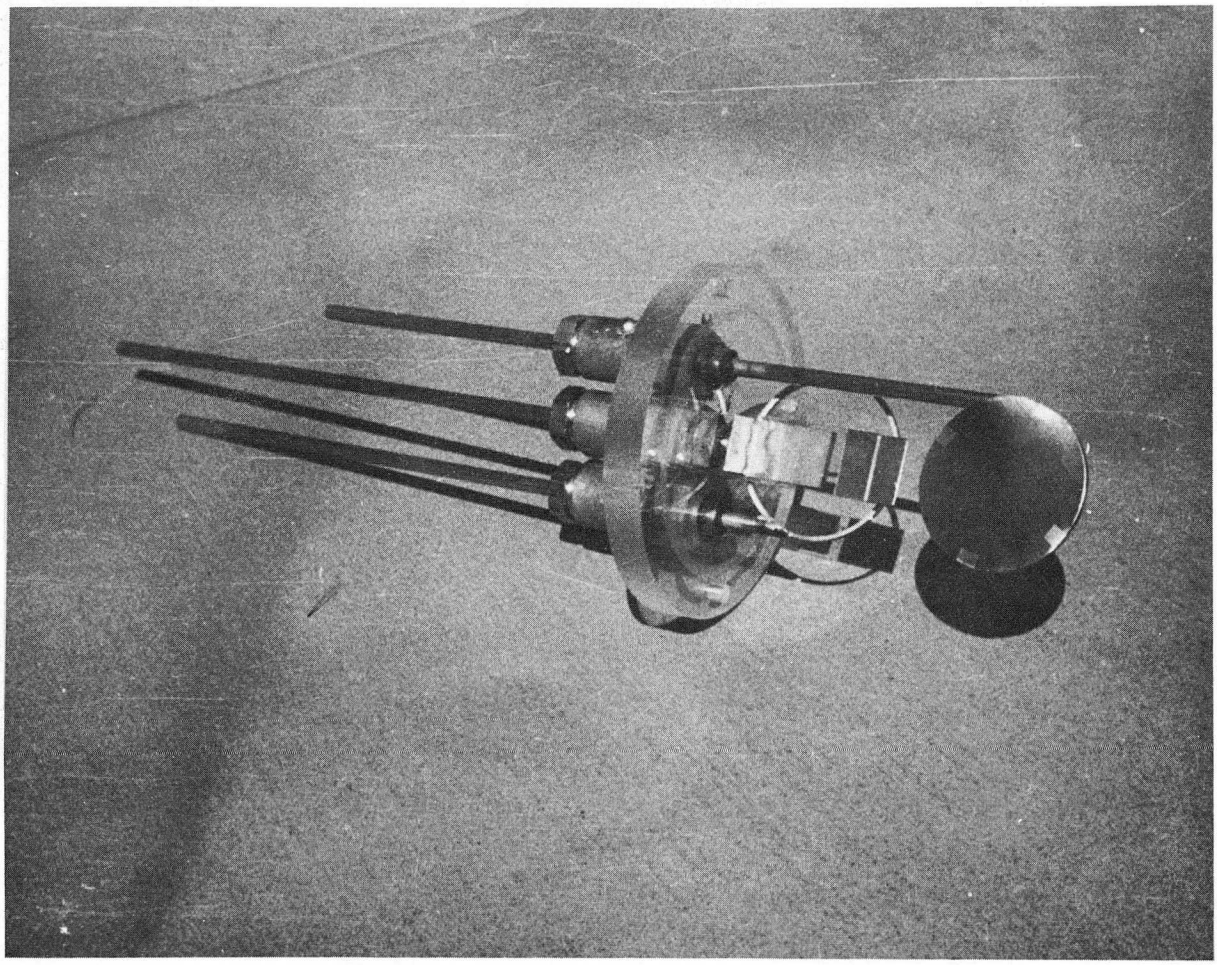

ZN-2281

Fig. 8. Target assembly removed from beam tube.

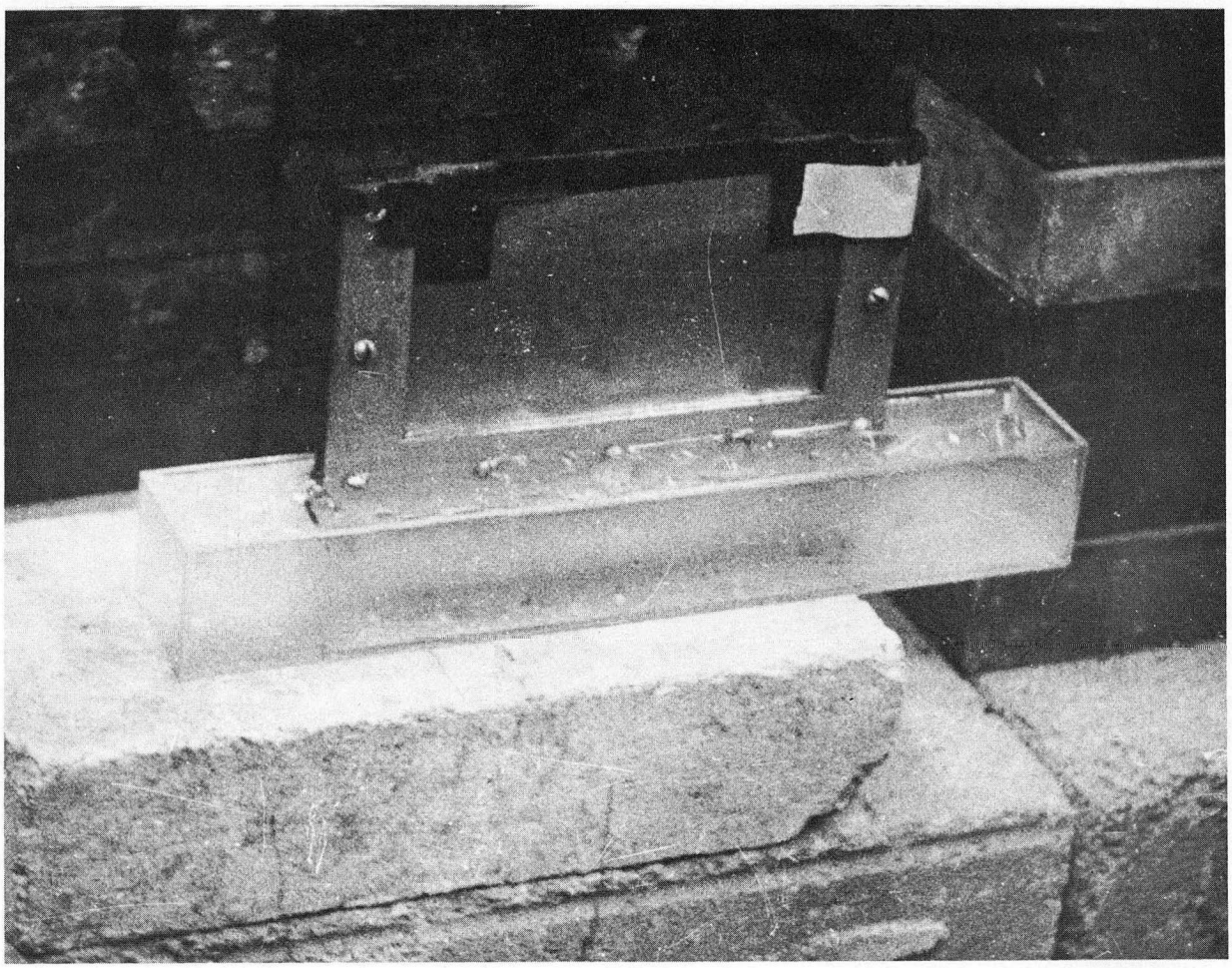

ZN-2284

Fig. 9. Plate holder. Beam enters from lower right.

of the plate holder were kept wet by the presence of an excess of D_2O or H_2O in their respective sections. The entire plate holder was cooled with ice water during exposure to reduce fading and to preserve the emulsion.

III. EXPERIMENTAL DETAILS

A. Choice of Basic Experimental Conditions: Detection Method, Energy, and Target

For photon energies of a few Mev the most convenient method of detection of polarization is the observation of the angular distribution of protons from the photodisintegration of deuterium. (Metzger and Deutsch have shown that the scattering asymmetry necessary to detect polarization by another possible method, Compton scattering, falls rapidly above a very few Mev.)[9] The maximum for the electric dipole photodisintegration cross section of deuterium occurs at a photon energy k of a little less than 5 Mev. Karplus and Reifman's computations,[10] on which the original planning of this experiment was founded, indicate that polarization increases as k/E_0 decreases. The approximations made in the papers on which their work is based (see Section IV-C-1) preclude allowing k/E_0 to decrease indefinitely, and $(k/E_0) = 1/5$ seems a safe limit. For this reason, and for convenience in comparison with other experimental work, some of which has been carried out at roughly that value, we chose the initiating electron total energy E_0 to be 25.5 Mev.

The following facts determined the choice of target: Karplus and Reifman point out that somewhat higher polarization (hence more easily detectable, as the measurement ultimately reduces to the subtraction of two large numbers) is to be expected for elements of low atomic number. One might think that the Z^2 dependence of the bremsstrahlung cross section would, from a practical point of view--the desirability of gathering data quickly--outweigh the points in favor of choosing a low Z. A dimensional analysis contradicts this:

If T is the thickness of the target in g/cm^2, and Σ_k is the whole-target cross section for bremsstrahlen of energy k, then, neglecting the log $Z^{-1/3}$ dependence, $\Sigma_k \sim Z^2 T/A$. The angle of maximum polarization for reasonably thin targets is close to $\theta_0 = mc^2/E_0$. The average root-mean-square spatial multiple-scattering angle is $\bar{a}_T \approx 2(mc^2/E_0)Z(T/A)^{1/2}$. In order that the multiple scattering in the target

not obliterate the polarization, we require $\bar{a}_T < \theta_0$. Take $\bar{a}_T = \theta_0/2$. Then $(T/A) = 1/(16\ Z^2)$ is a requirement on T/A. If we insert this target requirement in Σ_k, we see that under the conditions of this experiment the whole-target bremsstrahlung cross section is independent of Z !

The choice of target material is reduced to one of fixing upon a low-Z material which can be obtained in sufficiently thin foils with enough strength to hold together. Aluminum was chosen because of the ready availability of 1-mil foils--the appropriate thickness for that Z--of high purity.

More or less practical considerations thus governed the choice of experimental conditions. Although convenient experimentally, they unfortunately put the experiment in a region where precise theory is not yet available. The screening criterion on the basic cross section calculations determines this. For target Z = 13, the screening-criterion energy is $137\ Z^{-1/3}\ mc^2 \approx 30$ Mev. For complete screening total $E_0 \gg 30$ Mev; for no screening total $E_0 \ll 30$ Mev. This experiment lies between, in the region of partial screening. This complication is discussed in detail in Section IV-C-1.

B. Detection

The protons from the photodisintegration of deuterium were detected in Ilford C.2 emulsions as described in Section II-D. As this paper is not intended to be a dissertation on emulsion techniques, we mention here only certain problems peculiar to this experiment, and refer, for exhaustive treatments and references to the literature, to the review articles by Beiser[11] and Goldschmidt-Clermont,[12] on which we drew heavily.

Ilford C.2 emulsions were chosen for their appropriate sensitivity. More sensitive emulsions would have shown a greatly increased electron background fogging. Less sensitive emulsions might have been used, but the various necessary experimental abuses to which the emulsions were to be subjected in every case act to reduce sensitivity. As it happened, the proton tracks observed were for the most part at the limit of observability.

The emulsions were loaded with deuterium by soaking them in heavy water at room temperature for at least six hours prior to exposure, by which time they had absorbed essentially all the water they could. The background plates were loaded with ordinary water in the same way.

The water content of the emulsions was the principal limitation on their usefulness. It is generally known that fading of the latent image in emulsions used in the ordinary way is strongly dependent on humidity and temperature conditions to which they are subjected in the period between exposure and processing. Latent images are best preserved by keeping the emulsions cool and dry. When the plates are actually soaking wet, the rate of fading is increased by several orders of magnitude over that observed when the hygroscopic emulsions are treated more conventionally. The presence of moisture during exposure also decreases sensitivity.[13]

The fading effect can be somewhat retarded by keeping the emulsions cool. This was done experimentally by constructing the plate holder with a reservoir base. The reservoir was kept filled with ice water and the plates were cooled by conduction through the surrounding steel "sandwich" foils, whose bottom edges were in the reservoir(Fig. 9). (Stainless steel was chosen for the sandwich foils because, although it has a poorer heat conductivity than some other possible materials, it has appreciably less reaction with the surface of emulsions, as was proved in a subsidiary experiment.) The efficiency of this cooling method was proved in one run in an unfortunate way: the heavy-water-loaded plates froze, which shows that the sandwich was at or below 3.8° C.

The reduction of temperature during exposure also reduced sensitivity of the emulsion. While we have no data on this under our specific experimental conditions, it is to be expected that emulsions used more conventionally would lose roughly 20% of their sensitivity when cooled from room temperature to the freezing point.

Approximate calculations similar to those for growth curves in the bombardment-production of radioactive nuclei indicated that for our electron-beam intensity the increase in number photoprotons produced in the emulsion balanced the fading of latent tracks produced

earlier at an exposure time of about eight hours.

After that time the plates were immediately removed from the plate holder and development was begun on spot. Necessarily, there was some agitation due to the motion of the car carrying plates and experimenters to Berkeley, where processing of the plates was completed. This undoubtedly caused part of the surface fogging which hampered scanning.

C. Scanning and Analysis

A microphotometric measurement of the density of exposure of the emulsions determined the axis of the bremsstrahlen beam, and areas of the emulsions corresponding to various angles θ could thus be chosen for scanning. This procedure eliminates the effects of any slight misalignment of the apparatus or of stray field near the target, as all measurements--with the exception of the distance from radiator to emulsions--are on the plates themselves.

Proton tracks with ranges corresponding to photon energies between 3.6 and 9.7 Mev were accepted. In this energy range the photodisintegration of deuterium is almost wholly by electric dipole interaction; the magnetic dipole photodisintegration cross section is relatively very small. Experimental confirmation of the expected almost pure $\cos^2 \xi$ distribution of protons about the electric vector of plane polarized radiation in this energy range has been reported by Wilkinson[14] (ξ is defined immediately below). Earlier partial confirmation was exhibited by Hough[15] and by Gibson et al.,[16] who found close to a $\sin^2 \xi$ distribution of photoprotons about the propagation vector of unpolarized radiation.

It can be shown that if the distribution of protons in space about a fixed direction is $P(\xi)\, d\omega = (3/4\pi) \cos^2 \xi\, d\omega$, where ξ is the polar angle with respect to that direction, then the distribution of the projections of the proton paths on any plane containing the fixed direction is $N(\eta)\, d\eta = (1/\pi) \cos^2 \eta\, d\eta$, where η is the angle in the plane between the fixed direction and the projected path. If the plane chosen is that of the surface of the emulsion and the fixed direction

that of the electric vector, this corresponds to the data obtained by scanning. If we neglect the very small correction due to motion of the center of mass,[16] protons originating in the photodisintegrations induced by completely polarized radiation should have the projections of their tracks on the plane of the emulsion distributed as $\cos^2 \eta$ about the direction of the electric vector. The dip angle of a track in the emulsion is unimportant except in the determination of the range, hence acceptability, of the track. This is a lucky circumstance, as the dip angle is the hardest to measure precisely,[16] and is the only datum that must be corrected for shrinkage of the emulsion. (The soaking wet emulsions during exposure were about six times as thick as they were after development.) The projected angles do not change, whatever the shrinkage factor.

As stated above, a track was considered acceptable if its range corresponded to a photon energy between 3.6 and 9.7 Mev. The range in wet emulsion for a proton of energy corresponding to these photon energies is increased over that in dry emulsion by about 13%.[16] Acceptable ranges were determined by increasing the expected ranges of acceptable protons in dry emulsion[17] by this factor and calculating the limiting projected ranges and dips, the latter through knowledge of the swelling of the emulsion for a known water content.[13]

The data are lists of acceptable tracks in selected emulsion areas (corresponding to specific values of θ), and their projected angles. It can be shown that if $N_\perp$ and $N_{||}$ are the numbers of acceptable tracks in the quadrants (AOB) in Fig. 1, the experimental value of the degree of polarization to be compared with the theoretical prediction, Eq. (12) of Section IV-C-2, is

$$\Pi(\theta)_{exp} = \frac{\pi}{2} \frac{N_\perp - N_{||}}{N_\perp + N_{||}},$$

where $\pi/2$ is a geometrical factor. The modification of this expression to include background corrections is obvious.

Despite efforts to minimize the single-grain background in the plates, a combination of evils, principal among which were certainly Compton electrons produced by the bremsstrahlen and necessary rough handling of the emulsions, deposited a high density of single grains. Finding proton tracks could be compared to looking for an ill-defined constellation of stars in the brightest part of the Milky Way. This was true for both the D_2O- and the H_2O-loaded plates. Acceptable tracks were found at the rate of two or three per scanning day.

IV. THEORETICAL REMARKS

A. Plausibility Argument for Polarization

The theoretical justification for expecting bremsstrahlen to be polarized has been treated by several authors. For a survey of the theoretical work as it applies to this experiment, see Section IV-C. As an introduction, however, it would be useful to present a quasi-classical plausibility argument, based on the approach of Weizsäcker and Williams [18] and an appeal to the correspondence principle.

Consider an electron of energy $E_0 >$ a few mc^2, incident on a target nucleus, and moving along the x axis. The electron interacts with the Coulomb field of the nucleus, is accelerated, and produces in the process a photon. If we make a Lorentz transformation from the laboratory frame of reference, where the nucleus is at rest, to the frame of reference (designated by *) moving with the electron, the stationary electron in this frame "sees" approaching it in the $-x^*$ direction, with velocity v (Fig. 10), the Coulomb field of the nucleus, now much compressed by Fitzgerald contraction, i.e., a pulse of electromagnetic field. As in any frame a pulse of radiation of duration Δt contains a range of frequencies $\Delta\omega \sim 1/\Delta t$, this amounts to a pulse of virtual photons incident on the electron, some of which will be scattered.

We therefore expect Thompson scattering to occur. Fundamental to this description is the assumption that the influence of the Coulomb field on the electron is relatively weak. One pictures the virtual photons as gently "shaking" the electron in place, say along y^* (Fig. 10). Classically, this shaking results in induced electric dipole radiation by the electron, and we expect that in general the scattered radiation will be partly polarized. In particular, the radiation scattered into the y^*-z^* plane will be completely polarized, with $\vec{E}$ in that plane. Specifically, a wave whose propagation vector has one component, $\vec{k}_z{}^*$, will contain only $\vec{E}_y{}^*$ (Fig. 10). It is <u>only</u> in the y^*-z^* plane that complete polarization occurs. Radiation at angles other than $\pi/2$ to the x^* axis is only partly polarized, because other electrons in the incident beam pass other nuclei at various orientations; hence, for the whole incident beam, the shaking directions are uniformly

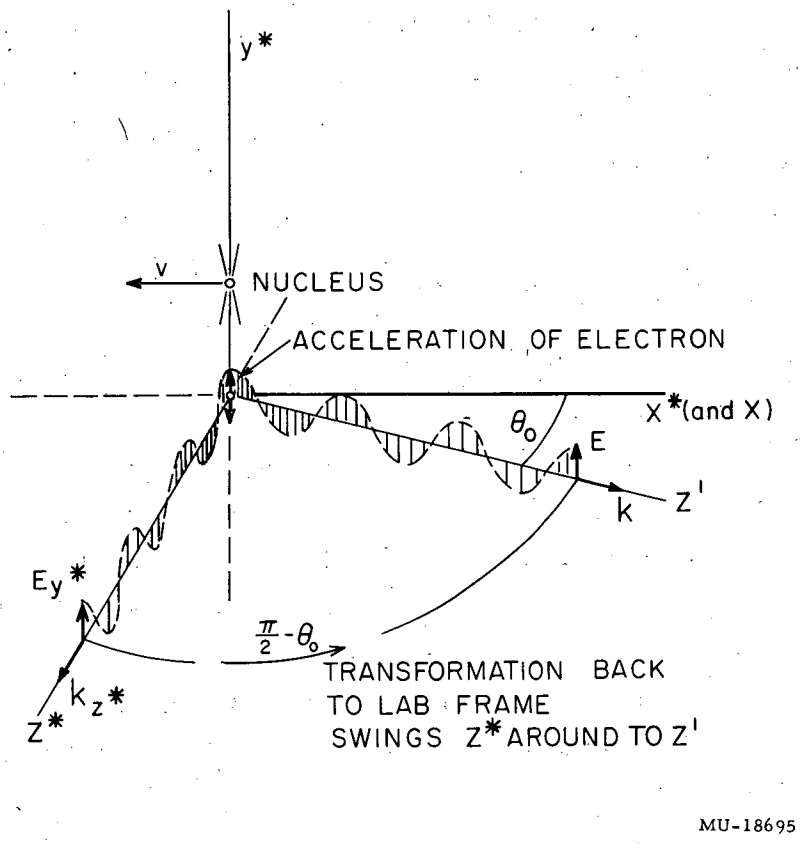

Fig. 10. Weizsäcker-Williams geometry.

distributed in the y^*-z^* plane, and the polarization of radiation not in that plane is not pure. For example, for the radiation with propagation vector along x^*, the polarization is zero.

If now we transform back to the laboratory system, the z^* axis becomes one generator, z', of the right circular cone about the x axis of half angle $\theta_0 = mc^2/E_0$. The whole y^*-z^* plane becomes the whole cone. In this simple picture, then, the radiation emitted on this cone is completely polarized in the sense introduced in Section I: $\vec{E}$ is everywhere tangent to the cone, i.e., the electric vector is perpendicular to the plane containing the path of the incident electron and the propagation vector of the scattered wave (in the special case of Fig. 10, the x-z' plane). In so simply described a case as this, we expect that while there may be modification in detail, precise calculation will approximate the correspondence-principle prediction that the polarization of bremsstrahlen (a) is in the sense described; (b) is greatest in the "wings" of the beam, at about θ_0; (c) is zero on the axis of the beam (for there there is no defining direction for the polarization); and (d) approaches zero again at large angles to the beam direction.

We should emphasize that the preceding argument applies only to the case of moderately high electron energy E_0 ($>$ a few mc^2) and to photons of energy somewhat below the upper limit of the bremsstrahlung spectrum, under which conditions the principal effect of the interaction on the motion of the electron in the laboratory system can be thought of as a transverse shaking superimposed on an undeflected trajectory. These are the conditions of this experiment.

Gluckstern and Hull have pointed out that for low incident energy and photon energy near the upper limit of the spectrum a curious reversal of the polarization occurs.[19] In such a case, we can apply purely classical concepts (no Lorentz transformation): In the non-relativistic limit, when the electron gives up most of its kinetic energy to the photon, so that the photon is near the upper energy limit of the spectrum, the acceleration of the electron is no longer a transverse shaking as above. Rather, the average acceleration of the electron is backward along the direction of motion. Because of the low electron energy, the nuclear influence is screened, and we now picture the

electron as merely slowing down in a dense medium. Again we have classical dipole radiation, but under these new conditions $\vec{E}$--which of course is parallel to the acceleration by the correspondence principle--is now in the plane of emission (the plane defined by the incident electron direction, hence $\vec{E}$ here, and the propagation vector of the photon), and the polarization under our definition approaches -1. This effect does not occur in the energy regions of interest in this experiment, where E_0 is high and $k \ll E_0$, but has been demonstrated experimentally for low E_0 by Motz and Placious.[5]

B. Remark on Plane vs. Circular Polarization

It is ordinarily assumed that quanta are circularly polarized, and that they have an angular momentum $1\hbar$ aligned either parallel or antiparallel to their propagation vector. How then can one speak of plane polarization for individual photons, the interactions of which are surely observed in the individual photodisintegrations measured? Indeed, if we were dealing with a pure beam of, say, right circularly polarized photons this would be a valid objection. Then, even classically, there is no preponderant plane polarization. But in general in the quantization of the electromagnetic field,[20] the quanta of which are photons, we obtain from the field amplitudes creation operators for, say, right and left circularly polarized photons which are related in phase. A canonical transformation of these operators changes them into new operators for plane polarized photons, also related in phase. That is, usually the photon is described by a mixed state. The measurement process is capable of annihilating only its own eigenstates, and therefore observes only the pure states to which it is sensitive with the probabilities described by the incident mixed state.

Lee and Yang[21] make a remark bearing on this: "The usual ways of measuring polarization through Compton effect, photoelectric effect, and photodisintegration of the deuteron are all incapable of detecting circular polarization. This is because circular polarization is specified by an axial vector parallel to the direction of propagation. From the observed momenta in these detection techniques such an axial

vector cannot be formed."

Aside from the question of the measurability of circular polarization with our techniques, another consideration of the fruitfulness of such a measurement applies. Recent interest in questions of parity conservation and related subjects has spurred a lively discussion in the literature of the precise description of polarization. Tolhoek[22] has shown that a complete statement of the state of polarization of photons requires three parameters (called Stokes parameters), which can be taken as the probability of circular polarization, and two probabilities of plane polarization whose reference planes make a dihedral angle of $\pi/4$. However, several investigators have pointed out that if the primary electron beam which generates the photons is itself unpolarized (as in this experiment), two of these probabilities of polarization of the photons--those of circular polarization and of plane polarization with respect to a reference plane at $\pi/4$ to the plane of emission--are exactly zero.[23-27] Consequently, the statement of the probability or degree of plane polarization as defined in this paper is, for the conditions of this experiment, a complete description.

C. The Theoretical Literature

1. The Intrinsic Cross Sections

At the time when this experiment was conceived, the intrinsic polarization of bremsstrahlen (hereafter, "intrinsic" means "single atom" or "ideally thin target") had been investigated in two principal theoretical treatments. Both essentially separated the Bethe-Heitler formula for the bremsstrahlung cross section[28,29] into polarized components. May considered the extreme relativistic case;[30] Gluckstern and Hull limited their treatment to the lower energy region.[19] The extent of their respective investigations and the approximations limiting the validity of each may be summarized as follows:

May

(a) Uses the Born approximation; $(Z/137\beta) \ll 1$: not valid for extreme upper end of photon spectrum

(b) Includes the effect of exponential screening on the intrinsic bremsstrahlung cross section: $E_0 \gg 137\, Z^{-1/3} mc^2$ for best prediction

(c) (From relativistic limitation) not valid for very soft quanta

Gluckstern and Hull

(a) Uses the Born approximation: not valid for extreme upper end of photon spectrum or for very low initial energy

(b) Neglects the effect of screening on the intrinsic bremsstrahlung cross section: $E_0 \ll 137\, Z^{-1/3} mc^2$

(c) (From neglect of screening) not valid for very soft quanta

Karplus and Reifman have compiled the theoretical predictions of these two investigations, and have plotted typical examples of each.[10] Their numerical calculation of the expected polarization as a function of the angle of emission of the photons and as a function of their energy for appropriate initial total energy E_0 was the specific inspiration for this experiment.

Since the experiment was performed, additional theoretical work has been published. In the two series of papers reviewed here, the starting point was again the matrix element from which is derived the Bethe-Heitler intrinsic bremsstrahlung cross section formula. Fronsdal and Überall extend the work of Gluckstern and Hull to include screening.[26] Olsen and Maximon use an entirely different approach.[27] The portions of these papers which apply to this experiment may be summarized according to the same points as above:

Fronsdal and Überall

(a) Uses the Born approximation: not valid for extreme upper end of photon spectrum

(b) Assumes exponential screening

(c) Has no limitation for soft quanta,

Olsen and Maximon

(a) Avoids the Born approximation: uses exact wave functions and determines the Coulomb correction. Not valid for extreme upper end of photon spectrum, however, because of neglect of terms $O(mc^2/E_{final})$

(b) Assumes Fermi-Thomas screening: exact

(c) Has no limitation for soft

as exponential screening is fitted to Fermi-Thomas results for complete screening	quanta due to a screening approximation, as that is treated exactly; however, terms $O(mc^2/k)$ are neglected

For the conditions of this experiment, the appeal of exactness in the treatment of the problem by Olsen and Maximon is somehwat vitiated by their neglect of terms of the order of mc^2/(electron energy: initial or final).[31] Also, Olsen, Maximon, and Wergeland have shown that the intrinsic electron bremsstrahlung cross section calculated in the Born approximation is only slightly modified by Coulomb corrections,[32] and Olsen and Maximon note that the intrinsic polarization-dependent cross sections have the same Coulomb (and screening) corrections as their previously found intrinsic cross section.[33,27]

Their Coulomb correction tends to reduce the prediction of degree of plane polarization slightly from that calculated in the Born approximation with screening only. However, because of the neglect of $O(mc^2/E)$ terms, the "exact" prediction is too low, at least for no screening.[4] It is not unreasonable, then, to take a Born-approximation-with-screening theory as the most useful for our experimental circumstances. May's theory involves certain relativistic approximations, and we are left with the extension of Gluckstern and Hull's work, now including screening by means of an exponential atomic form factor (and thus applicable to higher initial energies), reported by Fronsdal and Überall.

Their screening approximation is the same as that used by Schiff in his calculation of the intrinsic bremsstrahlung spectrum as a function of energy and angle.[34] Their open-form result for degree of polarization (Eq. (15) of Ref. 26) agrees with Gluckstern and Hull's for the case of no screening (their closed-form results--their Eq.(17)--involves the same approximation as Olsen and Maximon's results and is not considered here); and Gluckstern and Hull's total cross section agrees with Schiff's for the same case. As pointed out in point (c) above, the exponential screening approximation is exact for complete screening and for no screening, because the exponent is adjusted to agree with the Fermi-Thomas calculations for complete screening.

Having settled upon the exponential form-factor screening correction to the intrinsic cross sections, we must now consider the region of validity of this approximation under these experimental conditions. Three intrinsic cross sections are of interest: the two polarization-dependent cross sections, and their sum, the intrinsic bremsstrahlung cross section of Schiff. As noted above, Olsen and Maximon have shown that the screening corrections enter all three cross sections in the same way: therefore we need consider only Schiff's energy-angle distribution. In his theory the parameter $b = (2E_0 E\, Z^{1/3}/111\, k\, mc^2)$ measures the relative importance of screening: $b \ll 1$ corresponds to no screening; $b \gg 1$ corresponds to complete screening; and $(b/(x^2+1))^2 \geqslant 5$, where $x = \theta\, E_0/mc^2$, is a criterion for essentially complete screening for that portion of the radiation within the cone of half angle x. Even outside this cone, where the screening is incomplete, the exponential form factor gives an approximation to the correct distribution; within it the distribution is the same as that calculated with the Fermi-Thomas form factor. For these experimental conditions, $b = 8.7$, and the screening is essentially complete for radiation produced within the cone $x \leqslant 1.7$.

This is a mild restriction on the accuracy of our calculations. However, three considerations make it practically unimportant. (a) The theory is not far wrong outside this cone. (b) The intensity of the radiation per unit solid angle outside the cone is less than 7% of the central intensity. (c) The intensity of the radiation per unit solid angle on the cone for which $x = 1.7$ is 26% of that on the cone for which $x = 1$, where the polarization is at its maximum. If polarized bremsstrahlen are to be used experimentally, that portion of the beam most likely to be used is in the region of maximum polarization, $x = 1$.

2. Scattering in the Target: Mathematical Preliminaries and Definitions

Of the theoretical papers already mentioned, only May's includes--in addition to a discussion of the intrinsic cross sections—an estimate of the effect on the polarization of multiple scattering of the radiating electrons in a target of finite thickness. May makes use of Williams's multiple-scattering formula,[35] and combines with it the approximate Weizsäcker-Williams cross sections for bremsstrahlung. The limitations of his procedure are discussed below (Section IV-C-3).

In order to discuss May's estimate and others, and to develop one of our own, we need to define a terminology. For this we borrow heavily from Miller,[36] whose work is also discussed below.

Consider an electron of momentum $\vec{p}_0$ and total energy E_0 incident on a target of thickness T. Suppose the electron passes through a thickness $t < T$ and then radiates. We assume from the beginning that the target is thin enough that energy loss in transit is negligible: the electron's momentum at t, $\vec{p}_0'$, may differ from $\vec{p}_0$ in direction but not in magnitude. By the time the electron has reached t it has been scattered into a solid angle $d\Omega$ about the direction (α, ϕ), where $\alpha = (\vec{p}_0', \vec{p}_0)$ denotes the angle between $\vec{p}_0$ and the momentum after scattering, $\vec{p}_0'$. It is convenient to let $s = \alpha/\theta_0 = (\vec{p}_0', \vec{p}_0)$. See Fig. 11. (Hereafter, all angles except azimuthal angles, whether of scattering or of radiation, are measured in units of the characteristic angle of radiation $\theta_0 = mc^2/E_0$. Such reduced angles are designated by lower case roman letters.) Until Eq. (8) below, consider s fixed. Let the probability for scattering into $d\Omega$ be $f(s, \phi, t)\, d\Omega$. The radiation of momentum $\vec{k}$ is emitted in the direction $x = \theta/\theta_0 = (\vec{k}, \vec{p}_0')$; the cross section for this process is the intrinsic cross section for given E_0 and photon energy k per unit solid angle discussed above (Eq. (15) of Ref. 26). To keep clear the coordinates involved (Fig. 11) we designate this cross section as $d\sigma_{0i}'(x)$. (Hereafter, all cross sections and polarizations discussed in this paper are for unit solid angle, rather than the more common definition for unit angular interval.) The subscript 0 refers to the intrinsic cross section, the prime to the fact that the cross section is

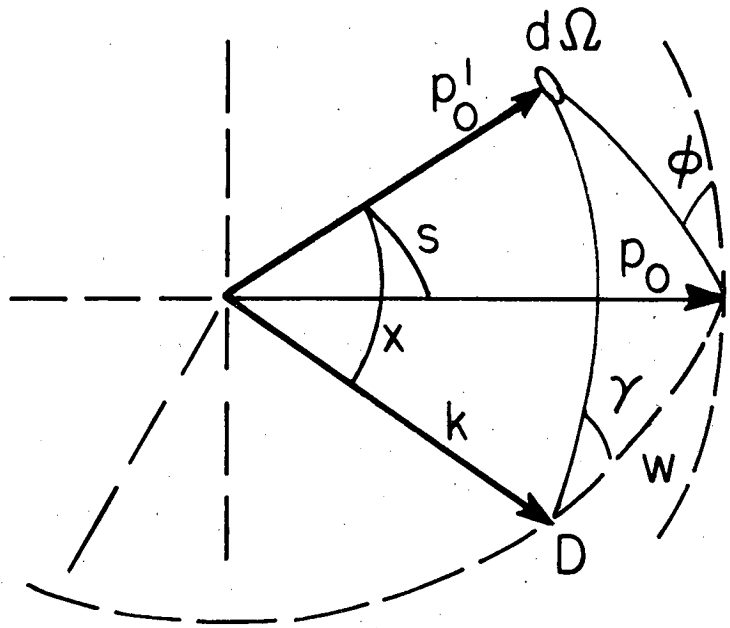

MU-18696

Fig. 11. Scattering and radiation angles. D corresponds to O in Fig. 1.

calculated in coordinates in which the $(\vec{k}, \vec{p}_0')$ plane is the plane of reference, and $i(=\perp, \parallel, BH)$ refers to the three cross sections of interest. $d\sigma'_{0BH}(x) = d\sigma'_{0\perp}(x) + d\sigma'_{0\parallel}(x)$ is the Bethe-Heitler or total intrinsic cross section. The probability of observing a photon of specified polarization ($i=\perp$ or $\parallel$), or of unspecified polarization ($i=BH$), whose origin was at t, at an angle $w=(\vec{k}, \vec{p}_0)$ with respect to the initial direction of the electron is the product of the probability $f(s, \phi, t)\ d\Omega$ and a number proportional to the cross section $d\sigma'_{0i}(x)$, where w and (s, ϕ) determine x uniquely.

Consequently, the total probability of observing such a photon at w is the product of these two probabilities integrated over the thickness of the target, and is proportional to

$$d\sigma'_i(x)\ d\Omega = \int_{t=0}^{t=T} d\sigma'_{0i}(x)\ f(s, \phi, t)\ dt\ d\Omega, \tag{1}$$

where $d\sigma'_i(x)\ d\Omega$ indicates the whole-target ith cross section for such photons referred to the $(\vec{k}, \vec{p}_0')$ plane. Because of the unique relationship among w, x, s, and ϕ, independent of t, this integral may be performed. Let

$$F(s, \phi, T)\ d\Omega = \int_{t=0}^{t=T} f(s, \phi, t)\ dt d\Omega. \tag{2}$$

Then Eq. (1) becomes

$$d\sigma'_i(x)\ d\Omega = F(s, \phi, T)\ d\sigma'_{0i}(x)\ d\Omega. \tag{3}$$

To repeat for clarity: Expression (3) is proportional to the number of photons arriving at point D (Fig. 11), of polarization i referred to the $(\vec{k}, \vec{p}_0')$ plane, originating from electrons which, anywhere in the target, have been scattered into the solid angle $d\Omega$ at (s, ϕ), and thereupon have radiated at such an angle x that they reach D.

Experimentally, the plane of reference is the $(\vec{k}, \vec{p}_0)$ plane. It should be noted that $\perp$ and $\parallel$ always refer to a specific reference plane. The direction $\parallel$, for example, is in general different in the primed and unprimed coordinates. It is a unit vector perpendicular to $\vec{k}$, lying in

the $(\vec{k}, \vec{p}_0')$ plane in primed coordinates, but in the $(\vec{k}, \vec{p}_0)$ plane in unprimed coordinates, and these two planes make a dihedral angle γ (Fig. 11). We must find, then, an expression that gives the contribution of photons of origin described above to the experimentally observed cross section.

Gluckstern, Hull, and Breit have remarked[24] that in general if ψ is the angle between the electric vector $\vec{E}$ and the plane of production of partly polarized radiation (here the $(\vec{k}, \vec{p}_0')$plane), the intrinsic cross section for radiation toward point D with $\vec{E}$ in the direction ψ, $d\sigma'_{0(\psi)}(x)$, is a function of the particular intrinsic cross sections $d\sigma'_{0i}(x)$:

$$d\sigma'_{0(\psi)}(x)=d\sigma'_{0\perp}(x)+(d\sigma'_{0||}(x)-d\sigma'_{0\perp}(x))\cos^2\psi. \tag{4}$$

From the geometry of Fig. 12, it is clear that $d\sigma'_{0(\psi)}(x)$ can be written in the unprimed coordinates $d\sigma_{0(\psi+\gamma)}(w)$. If we restrict $(\psi+\gamma)$ in the unprimed coordinates to the values $\pi/2(=\perp)$, and $0(=||)$, so as to conform with experimentally observed quantities, we thereupon express ψ in terms of γ, and, using Eq. (4), we get

$$d\sigma_{0i}(w) = R_{ij}(\gamma)\, d\sigma'_{0j}(x), \tag{5}$$

where

$$R_{ij}(\gamma) = \begin{pmatrix} \cos^2\gamma & \sin^2\gamma & 0 \\ \sin^2\gamma & \cos^2\gamma & 0 \\ 0 & 0 & 1 \end{pmatrix} \tag{6}$$

for $i, j = \perp, ||$, BH in the unprimed and primed coordinates respectively.

Because $F(s, \phi, T)$ is not a function of γ, Eq. (5) is applicable to the whole-target ith cross sections, too:

$$d\sigma_i(w) = R_{ij}(\gamma)\, d\sigma'_j(x), \tag{5a}$$

and, from Eq. (3),

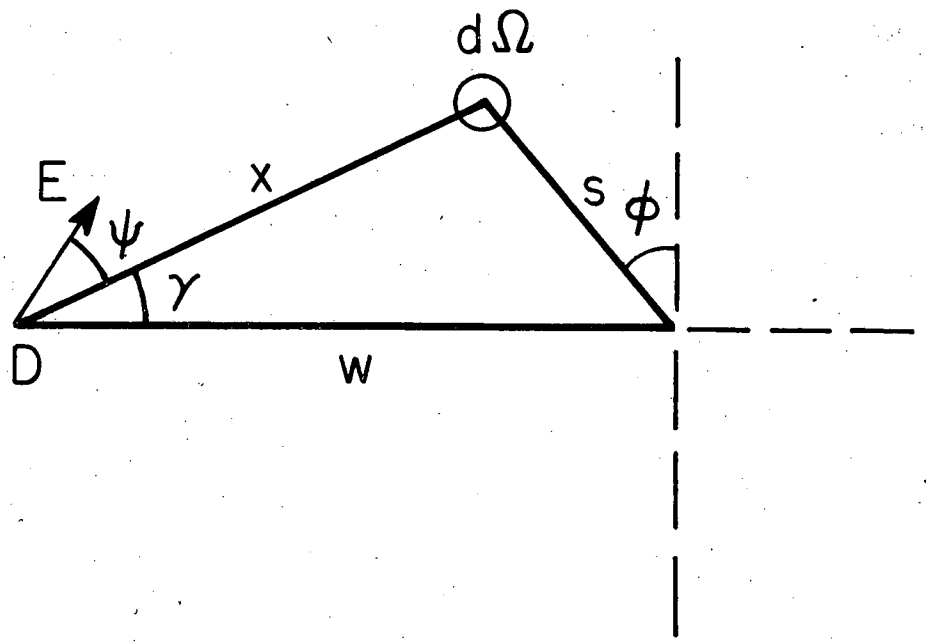

MU-18697

Fig. 12. View of Fig. 11 projected on the plane perpendicular to $\vec{p}_o$.

$$d\sigma_i(w)d\Omega = F(s, \phi, T)\, R_{ij}(\gamma)\, d\sigma'_{0j}(x)\, d\Omega. \tag{7}$$

Expression (7) is proportional to the number of photons arriving at point D, of polarization i referred to the $(\vec{k}, \vec{p}_0)$ plane, originating from electrons which, anywhere in the target, have been scattered into the solid angle $d\Omega$ at (s, ϕ), and thereupon have radiated at such an angle x that they reach D.

The total number of photons of polarization i defined in the laboratory frame is proportional to the contributions from Eq. (7) integrated over the solid angle:

$$\Sigma_i(w) = \int_\Omega d\sigma_i(w)d\Omega = \int_\Omega F(s, \phi, T)\, R_{ij}(\gamma)\, d\sigma'_{0j}(x)\, d\Omega. \tag{8}$$

The observed polarization, defined in the laboratory, is

$$\Pi(w) = \frac{\Sigma_\perp(w) - \Sigma_{||}(w)}{\Sigma_\perp(w) + \Sigma_{||}(w)} = \frac{\Sigma_\perp(w) - \Sigma_{||}(w)}{\Sigma_{BH}(w)}, \tag{9}$$

$$\Pi(w) = \frac{\int_\Omega F(s, \phi, T) \left\{ R_{\perp j}(\gamma) - R_{||j}(\gamma) \right\} d\sigma'_{0j}(x)\, d\Omega}{\int_\Omega F(s, \phi, T)\, d\sigma_{0BH}(x)\, d\Omega},$$

$$\Pi(w) = \frac{\int_\Omega F(s, \phi, T)(d\sigma'_{0\perp}(x) - d\sigma'_{0||}(x))\cos 2\gamma\, d\Omega}{\int_\Omega F(s, \phi, T)\, d\sigma_{0BH}(x)\, d\Omega}. \tag{10}$$

If we define the intrinsic polarization (we drop the subscript BH for the intrinsic bremsstrahlung cross section) by

$$\pi'_0(x) = \frac{d\sigma'_{0\perp}(x) - d\sigma'_{0||}(x)}{d\sigma_0(x)}, \tag{11}$$

then Eq. (10) becomes

$$\Pi(w, E_0, k, T) = \frac{\int_\Omega F(s, \phi, T)\, d\sigma_0(x)\, \pi'_0(x) \cos 2\gamma\, d\Omega}{\int_\Omega F(s, \phi, T)\, d\sigma_0(x)\, d\Omega}. \tag{12}$$

This is the theoretical prediction for observed degree of polarization in the laboratory frame in terms of the integrated scattering function $F(s, \phi, T)\, d\Omega$ of Eq. (2) and the theoretical intrinsic polarization and total cross section. The variables E_0, k, T are included as a reminder that all quantities under the integrals are functions of E_0, that the polarization and total cross section are functions of k as well, and that the total predicted polarization refers to that expected from a target of thickness T.

3. Scattering in the Target: Published Material

The first paper to discuss in detail the effect of scattering in the target on polarization was that of Miller.[36] The general approach through Eq. (4) in the preceding subsection is his. Miller, in reviewing May's work, shows that May has approximated the scattering in the target by assuming $F(s, \phi, T) = f(s, \phi, T)$, and taking for $f(s, \phi, T)$ Williams's multiple-scattering formula. This amounts to assuming that all the radiation occurs after the electrons have passed through the whole target, which is obviously a gross approximation. This overestimates the effect of multiple scattering, reducing the degree of polarization and spreading out the distribution in angle. The overestimation of the effect is compounded by May's use of Williams's scattering formula, which predicts a broader scattering distribution than is found experimentally.[37]

Miller reworks the problem, taking as his intrinsic cross sections the results of Gluckstern and Hull. Jamnik and Axel[4] have pointed out certain difficulties with this. First, there is a problem with the integral of Eq. (2), comment on which we defer to the section dealing with our own calculation. (Miller uses Williams's $f(s, \phi, t)$ and makes an approximate integral for $F(s, \phi, T)$: this represents his principal contribution.) Second, because Miller uses Gluckstern and Hull's formulae, he does not include the effect of screening, and therefore underestimates the divergence of the intrinsic bremsstrahlung angular distribution. Third, his method of averaging the contributions to the polarization from various regions of a thick target overestimates the observable polarization.

Jamnik and Axel's experiment used a betatron and an ingenious method for reducing the effect of multiple traversals of the target. However, they inferred an "effective target thickness" from experimental measurement of the angular distribution of bremsstrahlen and comparison with theoretical angular distributions from known targets. This lumps together the effects of actual multiple scattering in the target, beam divergence, and residual multiple traversals. Their "effective target thickness" was a reproducible two to three times the actual physical target thickness. While this is a consistent procedure for their experimental conditions, it does not say much about the details of scattering in the target.

We have found in the literature no satisfying theory involving adequate estimates of intrinsic polarizations and cross sections together with a reasonable approximation of the effect of scattering in the target. An attempt at such a treatment is set forth in the following section.

D. The Calculation of Expected Polarization, Including Scattering

To determine the expected polarization from a thin but finite target, such as was used for this experiment, we begin with Eq. (12), developed in Section IV-C-2:

$$\Pi(w, E_0, k, T) = \frac{\int_\Omega F(s, \phi, T) d\sigma_0(x) \pi_0'(x) \cos 2\gamma d\Omega}{\int_\Omega F(s, \phi, T) d\sigma_0(x) d\Omega} . \qquad (12)$$

We take $\pi_0'(x)$ to be given by Eqs. (15), (16a), and (16b) of Fronsdal and Überall's paper [26] ($\pi_0'(x)$ is their $P_{1in}^{(1)}$; x is their $\theta_1 E_1$); γ is defined by Fig. 12.

We take $d\sigma_0(x) \sim (1+x^2)^{-2}$. This requires discussion.

(a) Because $d\sigma_0(x)$ appears in both numerator and denominator, Eq. (12) is self-normalizing as far as constants are concerned.

(b) Under this approximation, the angle-dependent part of $d\sigma_0(x)$ is a function of E_0 (because $x = \theta E_0/mc^2$) but not of k; i.e., we assume the angular dependence of the intrinsic bremsstrahlung cross section to be

independent of photon energy. The k-dependent part of $d\sigma_0(x)$ cancels out in Eq. (12) along with the normalizing constants, hence need not be expressed. This is a good approximation to the Schiff intrinsic angular intensity distribution per unit solid angle, for fixed k (Schiff's Eq. (1) curly bracket),[34] as demonstrated by Lanzl and Hanson,[38] particularly for somewhat larger angles than fitted by their sum-of-two-Gaussians approximation.[31] The approximation becomes better as screening in the bremsstrahlung process becomes more nearly complete, as then the screening-dependent logarithmic term in Schiff's distribution becomes insensitive to angle x. Additional confidence in this approximation comes from Olsen and Maximon's work:[27] the dominant term in their total intrinsic energy-angle distribution per unit solid angle (their Eq. (7.2)) is precisely $(1+x^2)^{-2}$. Jamnik and Axel report very good agreement between this formula and their angular distribution of intensity from a platinum target.[4]

(c) It would of course be more consistent, inasmuch as we use Fronsdal and Überall's $\pi_0'(x)$, to use their values for $d\sigma_0(x)$. The reason this was not done is a purely practical one. Their expressions for the individual cross sections are extremely complicated, and this calculation was to be a manual one. Axel has generously supplied us with the intrinsic polarizations as a function of angle for the conditions of this experiment,[31] as calculated on the IBM-704 computer in Paris by using the CERN-2 program devised by Fronsdal and Überall, but the total intrinsic cross section is not at hand. However, the line of reasoning presented in the discussion of screening in the latter half of Section IV-C-1 suggests that our approximation (which has the advantage of previous experimental verification) is valid for Fronsdal and Überall's $d\sigma_0(x)$ as well.

$F(s, \phi, T)$ presents more of a problem. It was defined in Section IV-C-2:

$$F(s, \phi, T)\, d\Omega = \int_{t=0}^{t=T} f(s, \phi, t)\, dt\, d\Omega \qquad (2)$$

where $f(s, \phi, t)\, d\Omega$ is the (normalized) probability that an electron at $t < T$ in the target has scattered into a solid angle $d\Omega$ about (s, ϕ).

Much research has been done on the form of $f(s, \phi, t)$. Perhaps the two best-known treatments[39] are by Williams[35] and Molière.[40,41] The experiments of Hanson, Lanzl, Lyman, and Scott[37] and the analysis by Mohr and Tassie[42] confirm the accuracy of the Molière theory for thin foils. That theory predicts a distribution in angle of electrons emerging from a foil of thickness t which may be represented in series form. The first term is a Gaussian function; succeeding terms are corrections in inverse powers of a quantity B (of the order of 10 in magnitude), the solution of a transcendental equation. The leading correction term can be as much as 10% of the first term. Hanson et al.[37] have shown that the series may be represented by a single Gaussian function of width different from that of Molière's first term. In the notation of Ref. 41, Molière's first term 1/e-width is $B^{1/2}\chi_c$. Hanson et al. approximate the sum by a Gaussian function of 1/e-width $(B-1.2)^{1/2}\chi_c$. The quantity χ_c is determined by $\chi_c^2 = K_1(Z)\,\theta_0^2\,t$, where, for energetic electrons ($\beta \approx 1$), $K_1(Z)$ is a constant for a given target material. For aluminum, $K_1(13) = 4.06$ when t is expressed in g/cm^2.

What is of particular concern to us in this development is the variation of B with the thickness of the foil, as this knowledge is necessary for the integration of Eq. (2). For energetic electrons one finds $e^B/B = K_2(Z)t$, where $K_2(Z)$ is a constant for given target material. For aluminum, $K_2(13) = 7900$ when t is expressed in g/cm^2. In the region of useful target thicknesses, when t is doubled, B increases by about 18%, a relatively small change.

Equation (2) can be integrated conveniently only when B is a constant. For a target of thickness T, let B be evaluated for T/2.[43] Define

$$a_t^2 \equiv \frac{\chi_c^2(t)}{\theta_0^2}(B_{T/2} - 1.2) = K_1(Z)(B_{T/2} - 1.2)\,t = K_3 t. \tag{13}$$

Then, including the findings of Hanson et al., modified here by the use of $B_{T/2}$ as an effective B for the radiating electrons, we can approximate the Molière distribution by

$$f(s, \phi, t)\, d\Omega = (\pi\, \theta_0^2\, a_t^2)^{-1} \exp(-s^2/a_t^2)\, d\Omega, \tag{14}$$

and Eq. (2) becomes

$$F(s, \phi, T)\, d\Omega = (T/\pi\theta_0^2\, a_T^2)(-Ei(-s^2/a_T^2)), \tag{15}$$

where $(-Ei(-y))$ is given by Jahnke and Emde.[44]

Thus Eq. (12) becomes

$$\Pi(w, E_0, k, T) = \frac{\int_\Omega (-Ei(-s^2/a_T^2))(1+x^2)^{-2}\pi_0^{\perp}(x)\cos 2\gamma\, d\Omega}{\int_\Omega (-Ei(-s^2/a_T^2))(1+x^2)^{-2}\, d\Omega} \tag{16}$$

with (from Eq. (13))

$$a_T^2 = \frac{\chi_c^2(T)}{\theta_0^2}(B_{T/2} - 1.2). \tag{17}$$

This is the expression we calculate to find the predicted experimental polarization. It should be noted that this result holds for a perfectly collimated beam of incident electrons.

The quantity a_T is a reduced angle, the average root-mean-square spatial scattering angle, or the average 1/e-width of the scattering per unit solid angle, a measure of thickness of target, and corresponds to (but is not identical with) Miller's m. Miller used Williams's scattering theory, implicitly assuming log t was a constant over the target thickness. We expect the modified Molière-Hanson expression to provide a better estimate of the effect of scattering.

For our experimental conditions, a_T=0.320. The integration was done graphically with $0 \leq s \leq 2a_T$, which includes more than 98% of the scattered beam. The calculation, done for w = 1.5 only, involved 1997 algebraic operations, even with the rather gross approximation made ($d\Omega = 0.01\,\theta_0^2$), which indicates that further calculation would best be done by a computing machine.

V. RESULTS

Trustworthy results are disappointingly meager after so much work. Experience and a careful survey of the data lead one to the conclusion that it is inadvisable to combine scanning observations by different individuals. The plates in such an experiment are necessarily so dense that it is difficult to get agreement among observers on criteria for determining the existence of a track. It is necessary, then, that the same personal bias be present in all observations that are to be combined. Of course, personal bias contributes only to scanning efficiency, so that this restriction does not reflect on the reliability or reproducibility of final values for the degree of polarization, provided only that the same scanning efficiency applies to all data gathered for a given point. This is inherent in the expression for the degree of polarization: all the data are taken from the plates alone, as pointed out in Section III-C, and internal consistency is the only requirement on the scanning.

The only data that are wholly internally consistent are for $1.5\theta_0$, where the observed degree of polarization, when electrons of 25 Mev kinetic energy produce bremsstrahlen between 3.6 and 9.7 Mev in a 1-mil aluminum target, is $\Pi(1.5\ \theta_0)_{exp} = 0.44 \pm 0.22$. The probable error is given. This is to be compared with the theoretical prediction for these conditions (k=5 Mev assumed in the calculation), discussed in Section IV-D: $\Pi(1.5\ \theta_0)_{theor} = 0.45$.

The large error limits ascribed to this result arise principally from the appreciable background observed (about 45%). The result is calculated from a total of 444 acceptable tracks, observed in twelve months' scanning time. The background (observed in a congruent area of the H_2O-loaded emulsion) is mostly homogeneous, and probably arises from (γ, p) and (γ, n) -plus-knock-on processes in the other elements in the emulsion. For example, $O^{16}(\gamma, p)$ exhibits a resonance for the production of 2-Mev protons, which would be indistinguishable from protons from a deuteron photodisintegration by a photon with $k \approx 6.2$ Mev. Background measurements show a small asymmetry in a direction suggesting that we did not entirely eliminate neutron background

from the beam stopper.

Data were obtained by the same scanner (the author) at another azimuthal angle, also at 1.5 θ_0, from the D_2O-loaded emulsions (a total of 126 acceptable tracks). Because of time limitation, the corresponding background area was not scanned at this point. If the above remarks about the interpretation of the background are accepted, and the appropriate azimuthal angular adjustment of the background data applied to combine it with this additional material, and this is combined with the previously given results, one obtains $\Pi(1.5\ \theta_0)_{exp}$ = 0.32±0.12. It is reasonable that one should have less confidence in this than in the 0.44 experimental value, even though the calculated error is less, as there is no positive proof of the interpretation of the background data, nor solid justification for the adjustment applied to it.

Knowledge of the large background came rather late in the period of gathering data. A cursory survey of background plates had been made previously, leading to too small an estimate of background. Either the same scanners were unavailable or time did not permit a more careful background search; therefore many foreground data, gathered at 0.75 θ_0, 1.0 θ_0, and 2.5 θ_0, were discarded. The results reported earlier[6] were based on this work; it now appears that one should have little confidence in them, and they should be withdrawn.

The observational difficulties involved in this attempt to detect the polarization of bremsstrahlen are apparent. In further work it would seem that choice of a different method of detection would be desirable.

VI. ACKNOWLEDGMENTS

I wish to thank Professor A. C. Helmholz for suggesting this experiment, and for his counsel and patience; Dr. Walter H. Barkas for his guidance in the emulsion work and for the hospitality of his group; Drs. Robert W. Kenney and Fred W. Inman for their invaluable help in the performance of the experiment; Dr. Peter Axel of the University of Illinois for illuminating conversations about the theoretical analysis.

My deep appreciation goes also to members of the Hansen High Energy Physics Laboratory at Stanford University, particularly Dr. W. C. Barber, for the use of and help with the linear accelerator.

This work was done in part under the auspices of the U. S. Atomic Energy Commission.

REFERENCES

1. K. Phillips, Phil. Mag. 44, 169 (1953).
2. E. G. Muirhead and K. B. Mather, Australian J. Phys. 7, 527 (1954).
3. C. Tzara, Compt. rend. 239, 44 (1954).
4. D. Jamnik and P. Axel, University of Illinois Report: "Plane Polarization of 15.1-Mev Bremsstrahlung from 25-Mev Electrons," Urbana, Illinois, 1959.
5. J. W. Motz, Phys. Rev. 104, 557 (1956); J. W. Motz and R. C. Placious, Phys. Rev. 112, 1039 (1958).
6. Dudley, Inman, and Kenney, Phys. Rev. 102, 925 (1956).
7. W. K. H. Panofsky and J. A. McIntyre, Rev. Sci. Instr. 25, 287 (1954).
8. M. Camac, Rev. Sci. Instr. 22, 197 (1951); see also K. T. Bainbridge in Experimental Nuclear Physics, vol. 1, E. Segrè, ed. (John Wiley and Sons, Inc., New York, 1953), p. 566.
9. F. Metzger and M. Deutsch, Phys. Rev. 78, 551 (1950).
10. Robert Karplus and Alfred Reifman, "Polarization of Bremsstrahlung" UCRL-2686, September 1954.
11. A. Beiser, Revs. Modern Phys. 24, 273 (1952).
12. Y. Goldschmidt-Clermont, Ann. Rev. Nuclear Sci. 3, 141 (1953).
13. C. J. Batty, Nuclear Instr. 1, 138 (1957).
14. D. H. Wilkinson, Phil. Mag. 43, 659 (1952).
15. P. V. C. Hough, Phys. Rev. 80, 1069 (1950).
16. Gibson, Grotdal, Orlin, and Trumpy, Phil. Mag. 43, 457 (1952).
17. Walter H. Barkas and D. M. Young: Emulsion Tables I. Heavy-Particle Functions, UCRL-2579 (Rev), Sept. 1954.
    Barkas, Barrett, Cüer, Heckman, Smith, and Ticho: The Range-Energy Relation in Emulsion Part 1: Range Measurements, UCRL-3768, April 1957.
    Walter H. Barkas: The Range-Energy Relation in Emulsion Part 2: The Theoretical Range, UCRL-3769, April 1957.

18. C. F. v. Weizsacker, Z. Physik 88, 612 (1934); E. J. Williams, Phys. Rev. 45, 729 (1934); see also Ref. 29, p. 263.
19. R. L. Gluckstern and M. H. Hull, Jr., Phys. Rev. 90, 1030 (1953).
20. G. Wentzel, Quantum Theory of Fields (Interscience Publishers, Inc., New York, 1949), p. 111 ff.
21. T. D. Lee and C. N. Yang, Phys. Rev. 104, 254 (1956).
22. H. A. Tolhoek, Revs. Modern Phys. 28, 277 (1956).
23. Gluckstern, Hull, and Breit, Science 114, 480 (1951).
24. Gluckstern, Hull, and Breit, Phys. Rev. 90, 1026 (1953).
25. H. Banerjee, Phys. Rev. 111, 532 (1958).
26. C. Fronsdal and H. Uberall, Phys. Rev. 111, 580 (1958).
27. H. Olsen and L. C. Maximon, Phys. Rev. 114, 887 (1959).
28. H. A. Bethe and W. Heitler, Proc. Roy. Soc. (London) A146, 83 (1934).
29. W. Heitler, The Quantum Theory of Radiation, second ed., (Oxford University Press, London, 1944), p. 170.
30. M. M. May, Phys. Rev. 84, 265 (1951).
31. Peter Axel (University of Illinois), private communication.
32. Olsen, Maximon, and Wergeland, Phys. Rev. 106, 27 (1957).
33. H. Olsen, and L. C. Maximon, Phys. Rev. 110, 589 (1958).
34. L. I. Schiff, Phys. Rev. 83, 252 (1951).
35. E. J. Williams, Proc. Roy. Soc. (London) A167, 545 (1939).
36. J. Miller, C. E. N. (Saclay) Report C. E. A.-655: "Polarisation du rayonnement de freinage," n. d.
37. Hanson, Lanzl, Lyman, and Scott, Phys. Rev. 84, 634 (1951).
38. A. O. Lanzl and L. H. Hanson, Phys. Rev. 83, 959 (1951).
39. H. A. Bethe and J. Ashkin, in Experimental Nuclear Physics, vol. 1, E. Segre, ed. (John Wiley and Sons, Inc., New York, 1953), p. 282 ff.
40. G. Molière, Z. Naturforsch. 3a, 78 (1948).
41. H. A. Bethe, Phys. Rev. 89, 1256 (1953).
42. C. B. O. Mohr and L. J. Tassie, Australian J. Phys. 7, 217 (1954).
43. E. Hisdal, Phys. Rev. 105, 1821 (1957).
44. E. Jahnke and F. Emde, Tables of Functions (Dover Publications, New York, 1945), p. 6 ff.

This report was prepared as an account of Government sponsored work. Neither the United States, nor the Commission, nor any person acting on behalf of the Commission:

A. Makes any warranty or representation, expressed or implied, with respect to the accuracy, completeness, or usefulness of the information contained in this report, or that the use of any information, apparatus, method, or process disclosed in this report may not infringe privately owned rights; or

B. Assumes any liabilities with respect to the use of, or for damages resulting from the use of any information, apparatus, method, or process disclosed in this report.

As used in the above, "person acting on behalf of the Commission" includes any employee or contractor of the Commission, or employee of such contractor, to the extent that such employee or contractor of the Commission, or employee of such contractor prepares, disseminates, or provides access to, any information pursuant to his employment or contract with the Commission, or his employment with such contractor.